Central European Geology, Vol. 55/1, pp. 33–48 (2012)
DOI: 10.1556/CEuGeol.55.2012.1.3

Shock and thermal annealing history of the ALH 77005 Martian meteorite: a micro-Raman spectroscopical investigation

Szabolcs Nagy, Sándor Józsa
Eötvös Loránd University, Budapest

Arnold Gucsik*
Max Planck Institute for Chemistry Department of Biogeochemistry, Mainz, Germany

Szaniszló Bérczi
Eötvös Loránd University, Budapest

Kiyotaka Ninagawa
Department of Applied Physics, Okayama University of Science, Okayama

Hirotsugu Nishido
Research Institute of Natural Sciences, Okayama University of Science, Okayama

Miklós Veres
Research Institute for Solid State Physics and Optics Hungarian Academy of Sciences, Budapest

Ákos Kereszturi, Henrik Hargitai
Konkoly Thege Miklós Astronomical Institute, Research Centre for Astronomy and Earth Sciences Hungarian Academy of Sciences, Budapest

We studied optical microscopic and micro-Raman spectroscopic signatures of shocked olivine from the ALH 77005 Martian meteorite sample. The purpose of this study is to document pressure and temperature-related effects in olivine over the entire sample, which can aid in understanding structural changes due to shock metamorphism and the post-shock thermal annealing processes of lherzolitic Martian meteorites. According to the optical microscope observations, three areas may be discernible in olivine of the ALH 77005 in the vicinity of the melt pocket. The first area is the thermally undisturbed part of a grain, which contains a high density of shock-induced planar micro-deformations such as Planar Deformation Features (PDFs) and Planar Fractures (PFs). Compared to the first area, the second area shows less shock-induced microstructures, while the third area is a strongly recrystallized region, but not formed from a melt.

A common Raman spectral feature of these olivines is a regular doublet peak centered at 823 and 852 cm^{-1}; additionally, two new peaks at 535 and 755 cm^{-1} appear in the weakly annealed transition zones.

Key words: micro-Raman spectroscopy, shock metamorphism, olivine, Martian meteorite, high pressure zeta phase

Addresses: Sz. Nagy, S. Józsa, Sz. Bérczi, H. Hargitai: H-1117 Budapest, Pázmány Péter sétány 1/c., Hungary
Á. Kereszturi: H-1121 Budapest, Konkoly-Thege Miklós u. 14, Hungary
A. Gucsik: Hahn-Meitner Weg 1, D-55128 Mainz, Germany
H. Nishido, K. Ninagawa: 1-1 Ridai-cho, Okayama, 700-0005, Japan
M. Veres: H-1525 Budapest, PO Box 49, Hungary
*Corresponding author e-mail: ciklamensopron@yahoo.com
Received: December 5, 2011; accepted: January 24, 2012

Introduction

Olivine is one of the most refractory and abundant igneous rock-forming minerals, which has proved useful as an indicator of shock metamorphism in the study of meteorites (Stöffler 1972, 1974; Boctor et al. 1999; Langenhorst 2002; Chen et al. 2006). Thus, olivine has advantages compared to other minerals (e.g. plagioclase feldspar, pyroxene, etc.) that have been previously used as shock indicators, but are far less refractory than this mineral (Langenhorst 2002, and references therein).

Micro-Raman spectroscopy is a technique that allows information on the structure of the materials to be obtained from their characteristic vibrations (lattice vibrations in a crystal) from relatively small sample volumes (comparable to an electron microprobe). The resulting spectral bands depend upon the crystal structure with its symmetry, the vibrating atoms (with their masses) and the forces between them. This technique is a fairly routine one that is not too complicated in its application and could be useful for the identification and study of impact structures (Roberts and Beattie 1995, and references therein). However, only few Raman studies on naturally and experimentally shock metamorphosed olivine minerals from meteorites have been carried out so far (Farrel-Turner et al. 2005; Fritz et al. 2005a; Treiman et al. 2006).

The systematic studies of micro-Raman properties of experimentally shocked olivine crystal assemblages were performed by Farrel-Turner et al. (2005) and van de Moortéle et al. (2007). Farrel-Turner et al. (2005) found no significant characteristic relation between Raman shifts as a function of increasing shock pressure in olivine. However, van de Moortéle et al. (2007) described a new metastable phase formed at ambient pressure as the metastable intermediate during back-transformation from wadsleyite.

In this study we present the results of combined Optical Microscope and Raman spectroscopic observations performed on the Martian meteorite ALH 77005, in order to investigate the shock metamorphic history of lherzolitic shergottites.

Samples and experimental procedure

ALH 77005 Martian meteorite

The ALH 77005 Martian meteorite (lherzolitic type) was found in the area of the Allan Hills, South Victoria Land, in Antarctica in 1977–1978 by the U.S.–Japan meteorite search team (Yanai 1979). A preliminary examination of this sample reported that it contained 55% olivine, 35% pyroxene, 8% maskelynite, and 2% opaques. Olivine (Fo72) occurs as anhedral to subhedral grains up to 2 mm in length. The ALH 77005 consists of melt pockets, which are mostly crystallized as spinifex texture. Additionally, the interstitial regions contain two phases: pigeonite and residual glass (Harvey et al. 1993; McSween 1994; Ikeda 1998;

Mikouchi and Miyamoto 1998; Boctor et al. 1999; Nyquist et al. 2001). Olivine in the bulk of ALH 77005 is of brownish color (Ikeda 1994) and approximately 4.5 wt% of the total iron of the olivine is trivalent (Ostertag et al. 1984; Burns and Martinez 1991).

According to Nyquist et al. (2001), detailed investigations of lherzolitic textures revealed a preferred crystallographic orientation of olivine, proving that the lherzolitic shergottites are real cumulates, formed in a plutonic sub-surface environment (Berkley and Keil 1981; McSween 1994). Ikeda (1994) suggested that the compositional discontinuities among the four zoning types of chromite in ALH 77005 arise from magma mixing in shallow magma reservoirs on Mars. Their crystallization histories, as reconstructed by Harvey et al. (1993) and McSween (1994), require varying degrees of prolonged cooling to allow olivine to re-equilibrate at comparatively low temperature. On Earth, lherzolite crystallizes either at depths of >8 km (mantle rocks) or as cumulates in large magma chambers. Harvey et al. (1993) concluded that the trace element and minor element patterns of LEW 88516 and ALH 77005 minerals were essentially identical and consistent with large-volume, closed-system fractional crystallization followed by localized crystallization of isolated melt pockets.

Optical microscopy and micro-aman spectroscopy

The mineral assemblages and textures were characterized with a Nikon Eclipse LV100POL optical microscope. Raman spectra were recorded with a Renishaw Rm-2000 Raman spectrometer attached to a Leica DM/LM microscope. The 623 nm line with an Ar^+ laser served as excitation source; the laser power on the sample was 8 mW. The excitation beam was focused into a 1-μm diameter spot. Raman spectra were recorded in the 200–1100 cm^{-1} region using a CCD camera; the acquisition time was 60 sec. The polished thin sections of ALH 77005 sample were prepared at 35-μm in thickness. Two thin sections (ALH 77005-A and ALH 77005-B), which belong to the meteorite collections, were supplied by the National Institute of Polar Research (NIPR, Tokyo, Japan). They were mounted in the epoxy material. The ALH 77005-A thin section was used for the optical microscope investigations and Raman measurements were performed on the ALH 77005-B specimen. In general, ten Raman spectra were acquired per sample. In the present study, we show only one spectrum per sample, because the other spectra were identical. Intensity variations due to polarization effects were not observed.

Results

Optical microscope observations of olivine

In general, olivines in the ALH 77005-A sample are euhedral and subhedral minerals exhibiting mostly brownish color. Furthermore, coexisting Planar

Deformation Features (PDFs) with mosaicism (undulatory extinction) are discernible in all olivine grains. In our sample the olivine exhibits well-developed mosaicism showing reduced interference color. In the vicinity of the melt pocket, olivines can be divided into three regions as follows (Fig. 1). The first area is the farthest section of the olivine from the melt pocket, which can be characterized by a lower interference color (yellowish-orange). The second region is a transition zone containing planar microstructures and some isotropic area (Figs 1 and 2). The third section is a recrystallized area with patchy and irregularly rounded grains: this section neighbors the melt pocket. Those olivines, which are far from the melt pocket can be characterized with similar features as the "first area" mentioned in the earlier section.

The transition zone (located between the first and third sections described above) is about 20–25 μm wide (Fig. 2). In this section the interference color is significantly reduced, and some places show isotropic areas (Figs 1 and 2). Planar Deformation Features (PDFs) occur in up to two orientations in the transition zone. Additionally, Planar Fractures (PFs) show one orientation in this zone, in

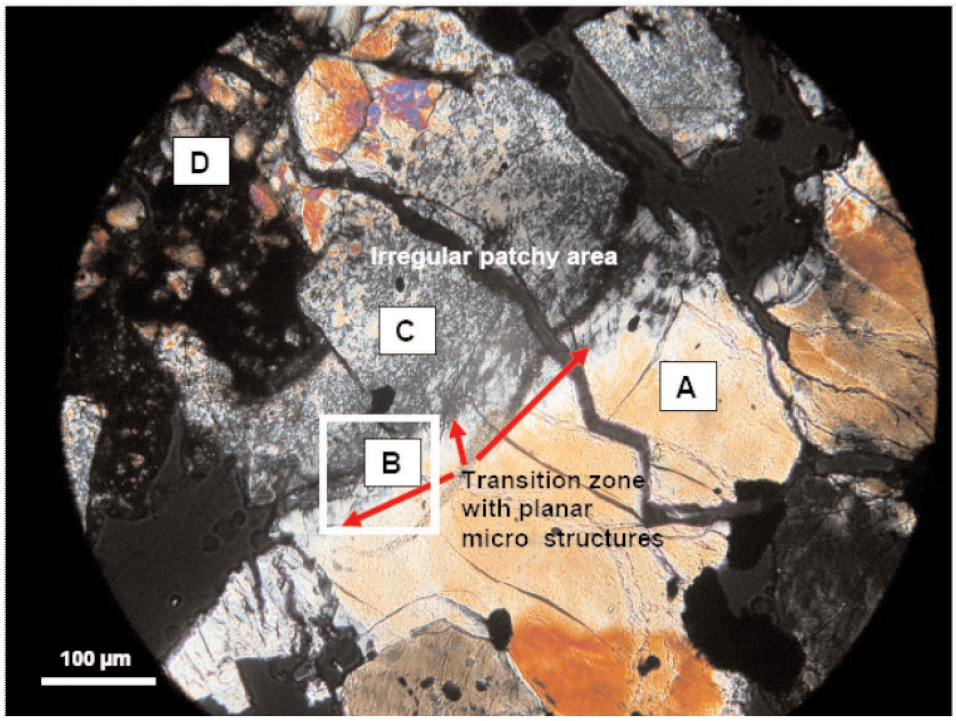

Fig. 1
Cross-polarized optical image of three different shocked regions of the ALH 77005-A thin section corresponding to the farthest section of the olivine from the melt pocket (A), transition zone with planar microstructures (red arrows-B), patchy irregular rounded grains (C), and melting pocket (D). The area within the white square is shown at higher magnification in Fig. 2

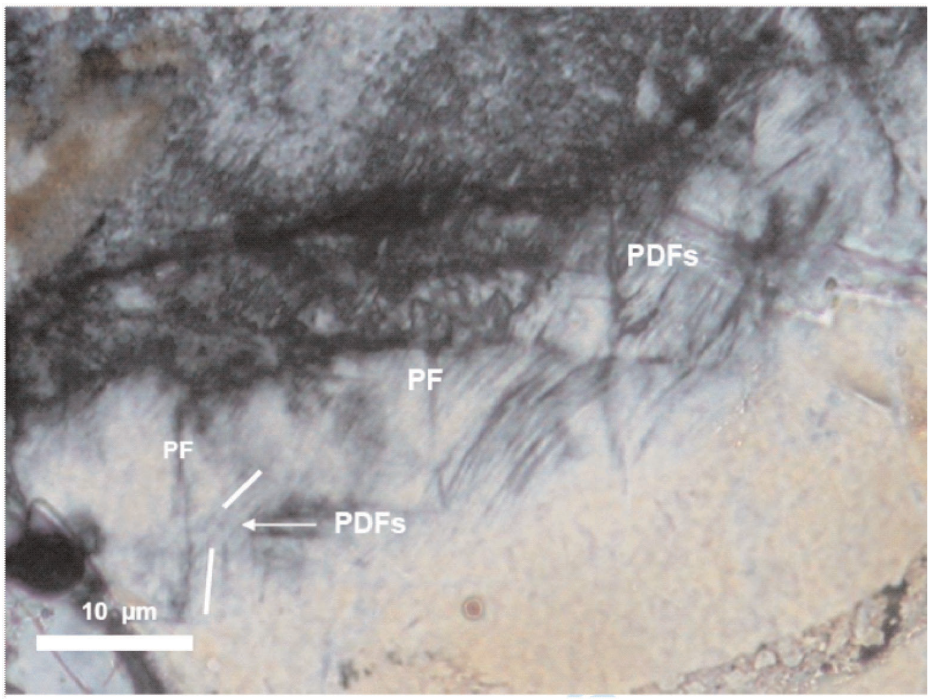

Fig. 2
Cross-polarized optical image of the transition zone (magnified from Fig. 1) showing two orientations (white lines) of PDFs in olivine

which the spacing of PFs is between 10 and 15 μm (Fig. 2). The PDFs are slightly curved, occurring between PFs. The width of PDFs is > 1 μm, and the spacing is 1–2 μm. The boundary between the transition zone and first section (with low interference color) is relatively sharp. However, the boundary region between the transition zone and the third section (recrystallized area) is continuous (Fig. 2). The olivine grains in the vicinity of the melt pocket have lost their intense brown color. It was observed that the olivine grains in the vicinity of the melt pocket do not exhibit pleochroism.

The third section as a recrystallized area exhibits the following texture. The second section is continuously transformed into this region, representing an irregular patchy area. It gradually grows into the melt pocket. This region contains several irregular olivine grains. Near the shock melt pocket, some of these olivine grains may have recrystallized from the melt pocket (Fig. 1).

In the vicinity of the melt pocket no shock veins are observed, and the number of fractures is relatively small. A high-pressure polymorph of olivine including spinel-type structure was not observed.

The ALH 77005 sample contains numerous mosaic-type textures in olivine grains (Fig. 3). In general the individual domains are of approximately 60×80 μm in size.

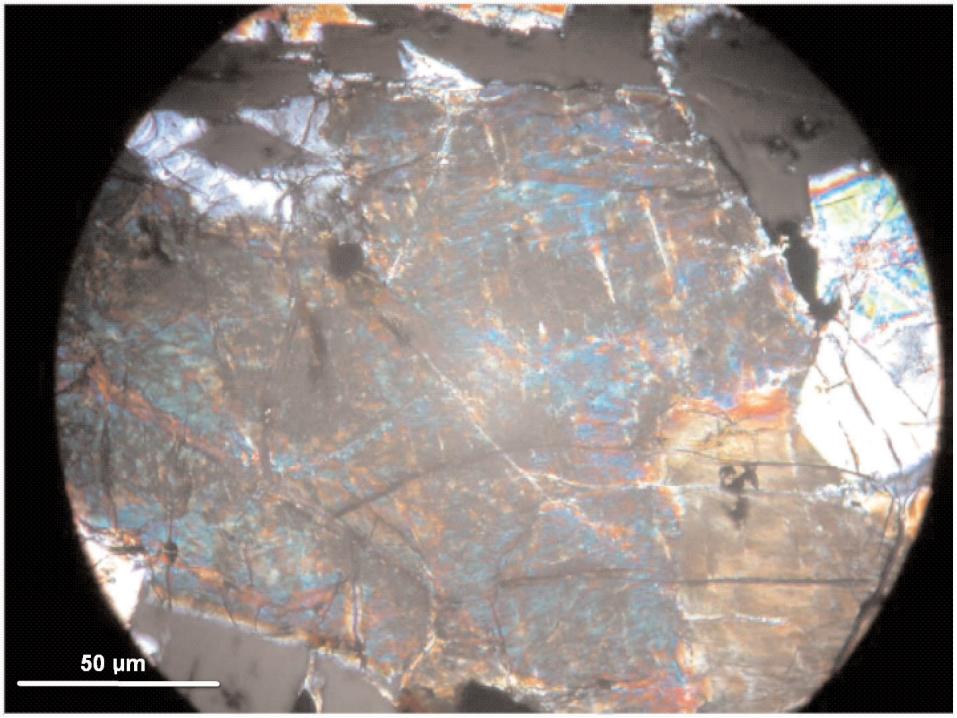

Fig. 3
The mosaic texture belongs to the high-shock pressure regime (scale: diameter of the selected area is 15 mm)

Raman spectra of olivine

There are grain-type belts from olivines around the melt pocket. The first belt of the grains is located close to the melt pocket containing three different optical zones. The size of these grains (ALH 77005-B) is about 1×1 mm (Fig. 1). The second grain belt lies between two melt pockets, but compared to the first grain belt it does not show different optical zones (approximately 3×2.5 mm in size). This part includes a relatively high density of PDFs. The third grain belt section is situated relatively far from the melt pocket; this dimension is 0.2×0.4 mm, and it shows stronger mosaicism and a higher density of PDFs than the second grain section. The distance of this third grain belt from the melt pocket is 4.5 mm and extends to the outermost boundary of the thin section.

The description of Raman properties of olivine grains was based on the increasing distance from the melt pocket to the outermost position of the sample, as follows. The first spectrum (sp1) is located in the nearest olivine grain belt to the melt pocket, and the fourth spectrum (sp4) lies at the farthest olivine grain belt from the melt pocket (Fig. 4). Between these regions of the sample, two

additional spectra were obtained (sp2 and sp3), which can be found in an intermediate location between spectra 1 and 4 (Fig. 4).

Close to the melt pocket, (sp1) olivine grains show the following Raman peaks: 311, 416, 600, 823, 853 and 957 cm^{-1}. In this spectrum all of the peaks contribute to the olivine structure. These spectral features correspond to the major olivine Raman peaks. However, the well-characterized olivine doublet proportion at 823 and 853 cm^{-1} is different from the unshocked olivine spectrum. The Raman spectrum of this site does not indicate significant changes in the olivine vibrational modes because it was overwritten by the heat annealing process of the melt pocket.

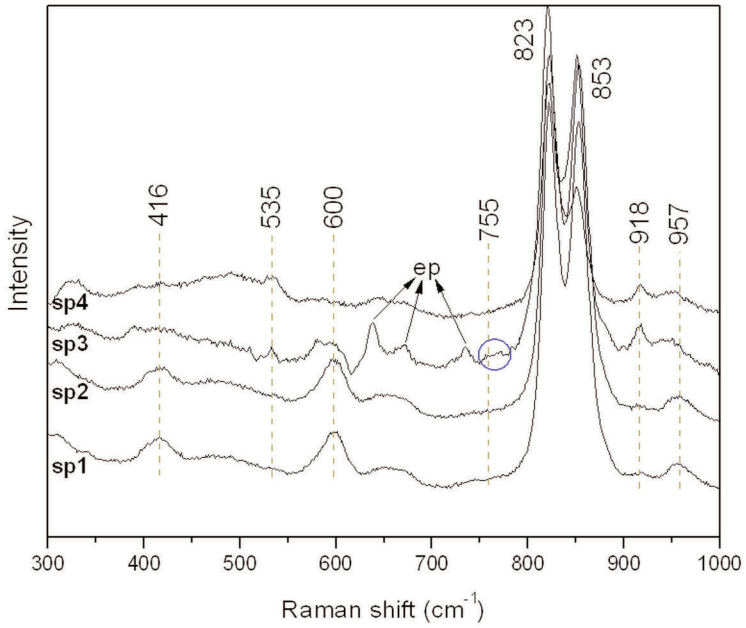

Fig. 4
Raman spectra of different distances of olivine grains from the melt pocket. Note: ep-corresponds to the Raman peaks of the epoxy material. The circle indicates a Raman band at 755 cm^{-1} of the sp3 spectrum

The intermediate region contains six Raman peaks: 416, 600, 755, 823, 853 and 957 cm^{-1}. In this spectrum (sp2) a new peak appears at 755 cm^{-1}. Furthermore, spectral features of this area exhibit slightly broadening features at the 300–600 cm^{-1} and 900–1000 cm^{-1}, which indicate the presence of a disordered state of the olivine.

The third spectrum (sp3) was obtained in the same grain as the sp2, but in the inner half of the olivine grain. The characteristic Raman peaks are the following: 535, 600, 823, 853, 916, 918 and 957 cm^{-1}. In the lower frequency modes (200–600

cm^{-1}) of this spectrum the main olivine Raman peaks disappear (416 cm^{-1}). The disappearance of the olivine-related peak at 600 cm^{-1} may indicate the presence of a new phase such as ξ–$(Mg, Fe)_2SiO_4$ (van de Moortéle et al. 2007). Additionally, there is a significant peak at 535 cm^{-1}. Three additional Raman peaks between 600 and 823 cm^{-1} correspond to the epoxy material. The position of the olivine doublet peak does not change, but its intensity ratio is smaller than in the previous two Raman spectra. Additionally a peak appears at 918 cm^{-1}, which is related to the major wadsleyite peak. However, the second major peak of wadsleyite at 712 cm^{-1} is absent. The peak at 957 cm^{-1} is also broadening, and it shifts to the low frequency range, which may be associated with the high shock stage in the interior of this olivine grain. As a summary, this (sp3) spectrum represents a mixed phase, which contains olivine, wadsleyite, and ξ-$(Mg,Fe)_2SiO_4$ phases because the peak at 535 cm^{-1} may be related to the ξ-$(Mg,Fe)_2SiO_4$ phase (this peak is related neither to α and β, nor to γ-olivine phases).

The fourth spectrum (sp4) contains five Raman peaks: 535, 823, 853, 918 and 957 cm^{-1}. This spectrum was measured in the farthest distance olivine grain belt from the melt pocket; therefore the heat annealing did not change the original structure of the olivine grains. The change of the ratio of the doublet peaks intensity is the most significant characteristic in this spectrum. The 918 cm^{-1} peak also appears in this spectrum. The most characteristic difference between (sp1), (sp2) and (sp3) spectra and the (sp4) spectrum is the absolute disappearance of the peak at 600 cm^{-1}.

The arrangement of the Raman spectra according to the increasing distance from the melt pocket corresponds to the optical microscopic observations. Both indicate a belt-like arrangement of the structural changes of olivine grains from the melt pocket away to its far regions. Relatively far from the melt pocket the olivine grains preserved stronger structural changes caused by the shock, and we could observe an intermediate area that was represented by spectras 2 and 3 with transitional structural changes characteristics.

Discussion

Shock-induced microdeformations of olivine

Shock-induced microdeformations in olivine have been described in samples from a variety of shock metamorphic environments including meteorites, terrestrial impact structures and shock recovery experiments. (i) In the low-shock pressure regime (5–18 Gigapascals (GPa)), olivine shows dislocation glide, the orientation of which depends on the shock front. (ii) Planar Fractures (PFs) and Planar Deformation Features (PDFs) in olivine are parallel to rational crystallographic planes (typically to low index planes), which occur between 5 and 52 GPa. (iii) According to Langenhorst (2002), both the internal fragmentation of olivine by fracturing and the high density of dislocations

contribute to the patchy extinction nature under crossed Nicols, known as mosaicism. (iv) Shock-induced recrystallization of olivine results in the formation of fine-grained and strain-free olivine aggregates, mainly in the shock veins (>45 GPa). (v) High-pressure phases of olivine are wadsleyite and ringwoodite occurring in the 1 μm-sized aggregates at shock stages between >35 GPa. However, production of glass such as diaplectic or shock-induced glasses have not been reported for olivine (Langenhorst 2002).

Mosaicism

The ALH 77005 sample contains numerous mosaic-type textures (Fig. 3) in olivine grains. According to Stöffler (1972, 1974) at some stage of shock intensity, olivine with planar fractures shows a distinctive mottled or mosaic appearance at extinction under the polarizing microscope. Single crystals display numerous, poorly-defined domains a few micrometers or less in size, which differ in their extinction positions by more than 30 to 50 of rotation. This causes the well-known shock-induced asterism observed in single crystal X-ray diffraction patterns. An important optical expression of mosaicism in our thin sections shows that each mosaic domain of the crystal still assumes a position of maximum extinction upon rotation; however, the crystal as a whole does not become absolutely dark at that position because the mosaic domains are much smaller than the thickness of the thin section. Therefore, numerous mosaic domains are superimposed on each other. The intensity of mosaicism, i.e. the number and disorientation of the domains, increases with increasing shock pressure, as documented by X-ray diffraction; however, this effect is difficult to quantify optically in thin sections (Stöffler et al. 1988)

High-pressure transformation of olivine

The high-pressure transformation of Mg-rich olivine to the more stable spinel or wadsleyite (ξ-Mg_2SiO_4) phases is kinetically inhibited at temperatures below 500 °C (Durben et al. 1993). TEM data on forsterite statically compressed to over 30 GPa and laser-heated to moderate temperatures (<700 °C) suggest an increase in disorder of the cation sublattice with increasing pressure and complete amorphization above 70 GPa (Durben et al. 1993). Shock compression data of forsterite suggest that the olivine structure persists up to 50 GPa, where the Hugoniot temperature is estimated to be 400 °C. It was also estimated that the olivine structure collapses (between 50 and 80 GPa) to an assemblage, which is ~20% denser than forsterite (Brown et al. 1987). The room-pressure density of spinel is only ~10% greater than forsterite. The observation of $MgSiO_3$ glass and MgO in forsterite samples recovered from shock pressures in excess of 100 GPa has been used to suggest that olivine decomposes to a perovskite and magnesiowüstite assemblage under dynamic compression (Durben et al. 1993).

Estimated shock stages of ALH 77005

The quantitatively estimated shock pressure of this meteorite such as 43±2 GPa was given by refractive index measurements of maskelynite (McSween and Stöffler 1980). More recently, Fritz et al. (2005b) provided a 45–55 GPa shock pressure estimation using appearance vesiculated maskelynite in meteorites. These observations indicate that olivines in ALH77005 were subjected to high pressure of approximately 50 GPa. Moreover, Fritz et al. (2005b) proposed a two-stage impact scenario for the lherzolitic shergottites: The launch-paired lherzolitic shergottite Y793605 is a monomict breccia, which can be argued to indicate an earlier impact that emplaced this rock on the surface of Mars. ALH 77005 could have been affected by the same impact event as Y793605. Thus, the lherzolitic shergottites (plutonic rocks) might have been emplaced on the surface of Mars by a first impact event, and were later ejected from the surface of Mars into space by a second impact. However, other scenarios are also possible (see Melosh 1984; Head et al. 2002; Artemieva and Ivanov 2004; Fritz et al. 2005b; Walton and Herd 2007 and references therein).

Brown and colorless meteoritic olivine

The brown color of the meteoritic olivine is commonly related to shock metamorphism and post-shock annealing processes. Recently, some studies have shown that shock-induced heating processes do not make olivine brown, because olivine from the highly metamorphosed terrestrial rocks is not brown (Treiman et al. 2006, and references therein). Taylor et al. (2002), Goodrich et al. (2003), and Herd (2006) found that brown olivine from the Martian meteorites is equilibrated at oxidizing (e.g. NWA 1068) and reducing (e.g. Dho 019, SaU005) states. Dyar et al. (1998) suggested that the heat-induced loss of hydrogen in olivine can also cause brown color in mantle nodules. Olivine can dissolve significant hydrogen, up to an equivalent of ~0.03 wt% H_2O in the Earth's mantle. H+ diffuses so quickly through olivine that it can be lost in a mild thermal event, and each H atom lost implies conversion of one Fe^{2+} to Fe^{3+}: H+olivine + Fe^{2+}olivine = ½[H_2]gas + Fe^{3+}olivine. For Earth mantle olivine, this yield of Fe^{3+} is ~1% molar of its total iron. The Fe^{3+} in olivine can remain in the lattice, charge-balanced by defects, or migrate to form crystalline inclusions of magnetite or magnesioferrite (Treiman et al. 2006, and references therein). This indicates that the ALH 77005 parent magma was hydrous when the olivine was crystallized. Alternatively, Puga et al. (1998) suggested that a preshock metamorphic event, below oxidizing conditions, may have produced tiny (less than 1 μm) magnetite exsolutions in ALH 77005 olivine crystals, which would be responsible for their brown color or would contribute to it.

Raman spectral characteristics of structural changes of olivine due to high pressure and temperature

Structurally, olivine is an orthosilicate with isolated SiO_4 tetrahedra. Kuebler et al. (2005) identified 81 optic modes, 36 of which are Raman active modes in olivine, which can be divided into three groups: (1) less than 400 cm^{-1}, which corresponds to the lattice modes (rotations and translations of SiO_4 units, and translations of the octahedral cations). (2) 400–800 cm^{-1}, which are related to the SiO_4 internal bending vibrational modes. (3) 800–1100 cm^{-1}, which is attributed to SiO_4 internal stretching vibrational modes.

Peaks at 820 and 850 cm^{-1}: The dominant features in the high Raman frequency region of olivine (800–1100 cm^{-1}) are the doublet peaks at 820 and 850 cm^{-1} (Fig. 4), which are related to SiO_4 internal stretching vibrational modes. It was reported that the doublet peak positions change as a function of variation of the chemical composition (Kuebler et al. 2005). In our sample, the change of the intensity ratio of this peak as a function of the increasing distance from the melt pocket to the outer parts of the sample is associated with the presence of shock metamorphic effects. This indicates that the region of sp1 has been affected by the strongest shock after the melt pocket. It is also demonstrated that during the melt pocket forming, the primary shock effects did not survive the heat annealing process; thus the olivine structure might have been rebuilt in this region.

Peak at 755 cm^{-1}: This peak was described both in the experimentally shocked and in natural samples (Durben et al. 1993; Gillet et al. 2005; van de Moortéle et al. 2007). These authors suggested that this peak may be associated with the SiO_5 and SiO_6 molecules as "defects within the olivine structure" (Durben et al. 1993; van de Moortéle et al. 2007). However, alternatively, Gillet et al. (2005) suggested that the peak near at 750 cm^{-1} might be attributed to the presence of Si-O-Si bridges characteristic of wadsleyite.

Peak at 535 cm^{-1}: van de Moortéle et al. (2007) suggested that this peak is attributed to a new ξ-$(Mg,Fe)_2SiO_4$ phase indicating metastable back transformation of wadsleyite at high shock pressures. This peak is a newly observed Raman peak in this study.

Table 1 summarizes the major Raman spectral features of the high-pressure olivines in NWA 1950 and NWA 2737 observed in previous studies (Gillet et al. 2005; van de Moortéle et al. 2007). Transformation of olivine to ringwoodite was not detected, probably because of the short duration of the shock, and because of the grains size as well as texture variation (Fritz et al. 2005b). Although this transformation in the ALH 77005 sample would have been highly probable because of the peak shock pressure and postshock temperature range of 45 to 55 GPa, and at least 2000 °C (Fritz et al. 2005a), which are enough for the ringwoodite formation.

Table 1
Observed transitional peaks corresponding to the high pressure transitional phases of olivine in different lherzolitic shergottites

Shock stage	Lherzolitic shergottite	Wavelength of the observed transitional peak in olivine	Observed transitional peak in olivine	Observed wadsleyite peak
S6: 45–55 GPa	ALH-77005	In this study 751 cm^{-1}	In this study 535 cm^{-1}	In this study 918 cm^{-1}
S5: 35–45 GPa	NWA 1950	Gillet et al. 2005 754 cm^{-1}		
S3: 20–25 GPa	NWA 2737 Low T.	Van de Moortéle et al. 2007 760 cm^{-1}		

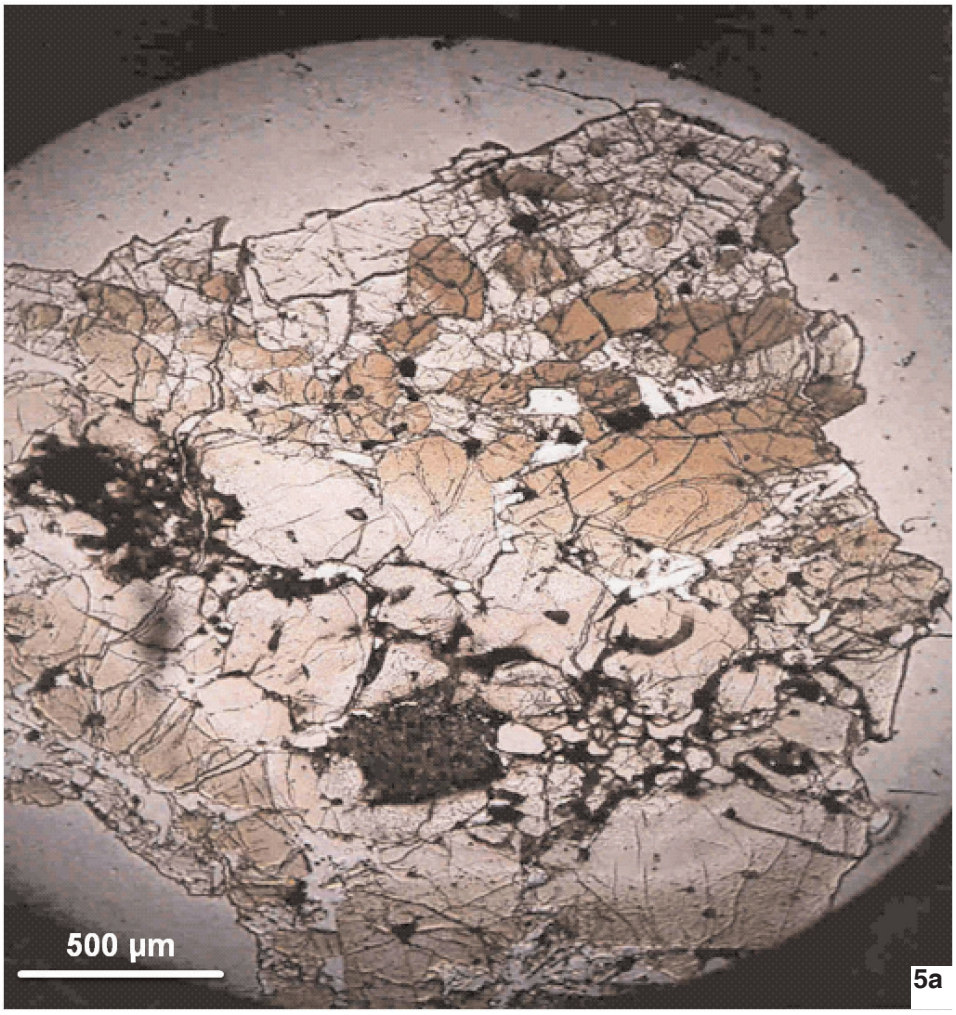

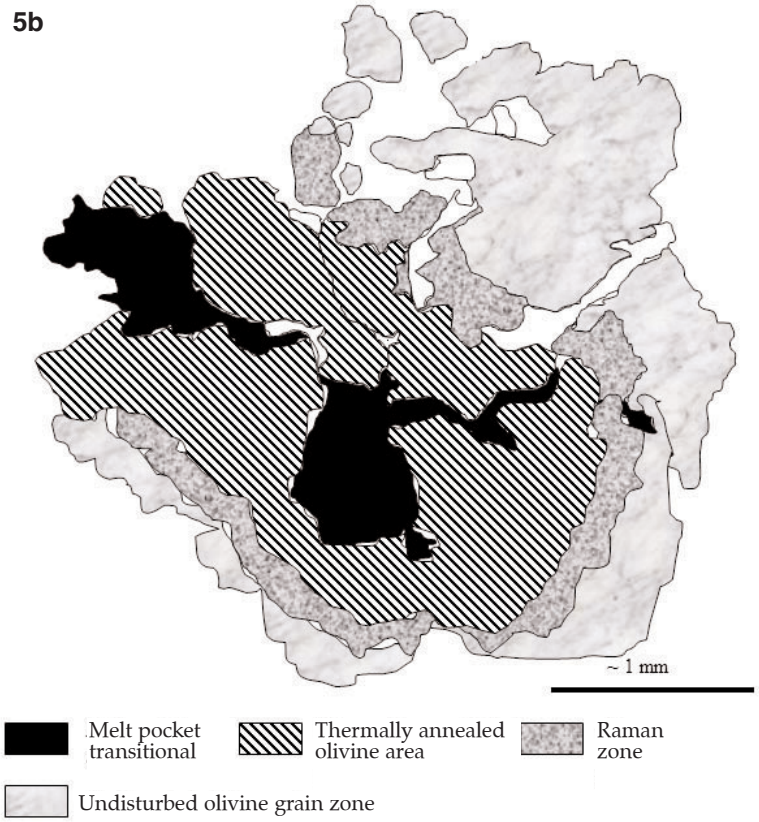

Fig. 5
← a. OM image of the region of the ALH 77005-B thin section: overview (plane polarized light).
b. Sketch of the structural zones surrounding the melt pocket region of the ALH 77005 thin section based on the optical and Raman spectral studies. The dark region indicates the melt pocket, the surrounding innermost zone belongs to the annealed olivines. Next is the mixed (probably mosaic-like) olivine phase zone with two types of additional Raman peaks (535 and 755 cm^{-1}): this zone was partially annealed. The outermost zone contains wadsleyite Raman peaks: this region was not subjected by the thermal annealing process

An optical image (Fig. 5a) and a sketch of the band-like arrangement of the shock metamorphic features obtained by micro-Raman spectroscopy can be found in Figure 5b.

Conclusions

This paper reports on optical microscopy and micro-Raman spectroscopic investigations of olivine from the Martian meteorite ALH77005. Texturally different olivines, which differ in their distances to large melt pockets, were studied.

Our combined optical microscopy and micro-Raman spectroscopy studies of olivines in the ALH 77005 Martian meteorite revealed the multiple effects of high pressure and melting during the shock metamorphic process. Mechanical crystal deformations at high pressure in olivines are PF and PDF, which can be found all over the thin sections, except in those localities where they decrease in number and become extinct because they were annealed by the heat effects in the vicinity of the melt pockets.

By additional as well as missing Raman peaks, the olivines predict the counterplay of the shock pressure and the annealing effects of the high temperature near melt pocket. The Raman spectra demonstrate zones around a melt pocket designated as band-like regions. The high-pressure transitional states were found in two forms. The first was characterized by a peak at 535 cm^{-1} and the other shows one at 755 cm^{-1}. This gradual appearance of the new phase inside the lower-pressure regime opens the possibility of summarizing the interplay of barometric and annealing effects on olivine.

These results show a clear dependence of the Raman properties of olivine with the combined effect of shock pressure and the vicinity to the annealing heat centers (melt pockets). The gradation of the micro-Raman spectra along the line from the melt pocket to the undisturbed regions of the sample also suggests a method of an olivine shock barometry. This gradation depends on the existing normal peaks, the missing and the extra peaks of the olivine micro-Raman spectra.

Further studies may also focus on the combination of missing and additive Raman peaks and their connection with other crystallographic methods to show various other combinations of heat and pressure in highly shocked olivine regions in Martian meteorites.

Acknowledgements

This study was supported by the international joint collaboration of JSPS-HAS (No. 2007/104.). The authors are grateful to Dr. H. Kojima for the loan of the Antarctic Meteorite set (NIPR, Tokyo, Japan). They are also grateful for the useful comments on this manuscript given by Drs. A. Wang, J. Fritz and U. Ott. Finally, they wish to express their thanks to Dr. habil. Zuárd Ditrói-Puskás for his review of this paper.

References

Artemieva, N.A., B. Ivanov 2004: Launch of Martian meteorites in oblique impacts. – Icarus, 171, pp. 84–101.

Berkley, J.L., K. Keil 1981: Olivine orientation in the ALHA 77005 achondrite. – American Mineralogist, 66, pp. 1233–1236.

Boctor, N.Z., Y. Fei, C.M. Bertka, C.M.O.D Alexander, E. Hauri 1999: Shock metamorphic effects in Martian Meteorite. – ALHA 77005 (abstract #1628). 30th Lunar and Planetary Science Conference. CD-ROM.

Burns, R.G., S.L. Martinez 1991: Mössbauer spectra of olivine-rich achondrites: Evidence for preterrestrial redox reactions. – Proc. Lunar Planet. Sci. Conf. 21st, Lunar and Planetary Institute, Houston, pp. 331–340.

Brown, J.M., M.D. Furnish, R.D. McQueen 1987: Thermodynamics for $(Mg,Fe)_2$ SiO_4 from the Hugoniot. – In: Manghnani, M.H., Y. Siono (Eds): High pressure research in mineral physic.s American Geophysical Union, Washington, D.C., pp. 373–384.

Chen, M., H. Li, A. El Goresy, J. Liu, X. Xie 2006: Intracrystalline transformation of olivine to ringwoodite in the Sixiangkou meteorite (abstract#5006). – 69th Annual Meteoritical Society Meeting. CD-ROM.

Durben, D.J., P.F. McMillan, G.H. Wolf 1993: Raman study of the high pressure behavior of forsterite (Mg_2SiO_4) crystal and glass. – American Mineralogist, 78, pp. 1143–1148.

Dyar, M.D., J. Delaney, S.R. Sutton, M. Schaefer 1998: Fe^{3+} Distribution in oxidized olivine: A synchrotron micro-XANES study. – American Mineralogist, 83, pp. 1361–1365.

Farrel-Turner, S., W.U. Reimold, U. Nieuwoudt, R.M. Erasmus 2005: Raman spectroscopy of olivine in dunite experimentally shocked to pressures between 5 and 59 GPa. – Meteoritics and Planetary Science, 40, pp. 1311–1327.

Fritz, J., A. Greshake, D. Stöffler 2005a: Micro Raman spectroscopy of plagioclase and maskelynite in Martian meteorites: Evidence of progressive shock metamorphism. – Antarctic Meteorite Research, 18, pp. 96–116.

Fritz, J., N. Artemieva, A. Greshake 2005b: Ejection of Martian meteorites. – Meteoritics and Planetary Science, 40, pp. 1393–1411.

Gillet, P., J.A. Barrrat, P. Beck, B. Marty, R.C. Greenwood, A. Franchi, N. Bohn, J. Cotten 2005: Petrology, geochemistry, and cosmic-ray exposure age of lherzolitic shergottite Northwest Africa 1950. – Meteoritics and Planetary Sciences, 40, pp. 1175–1184.

Goodrich, C.A., D. van Niekerk, M.L. Morgan 2003: Northwest Africa 1110: A New Olivine-Phyric Shergottite Possibly Paired with Northwest Africa 1068 (abstract#1266). – 34th Lunar and Planetary Science Conference. CD-ROM.

Harvey, R.P., M. Wadhwa, M.Y. McSween, Jr., G. Crozaz 1993: Petrography, mineral chemistry and pertogenesis of Antarctic shergottite LEW88516. – Geochimica and Cosmochimica Acta, 57, pp. 4769–4783.

Head, J.N., H.J. Melosh, B.A. Ivanov 2002: Martian meteorite launch: High-speed ejecta from small craters. – Science, 298, pp. 1752–1756.

Herd, C.D.K. 2006: Insights into the redox history of the NWA 1068/1110 martian basalt from mineral equilibria and vanadium oxybarometry. – American Mineralogist, 91, pp. 1616–1627.

Ikeda, Y. 1998: Petrology of magmatic silicate inclusions in the Allan Hills 77005 lherzolitic shergottites. – Meteoritics and Planetary Science, 33, pp. 803–812.

Ikeda, Y. 1994: Petrography and petrology of the ALH 77005 shergottite. – Proceedings of NIPR Symposium of Antarctic Meteorite Research 7, pp. 9–29.

Kuebler, K., B.L. Jolliff, A. Wang, L.A. Haskin 2005: Extracting Olivine (Fo-Fa) Compositions from Raman Spectral Peak Positions (abstract#2086). – 37th Lunar and Planetary Science Conference. CD-ROM.

Langenhorst, F. 2002: Shock metamorphism of some minerals: Basic introduction and microstructural observations. – Bulletin of Czech Geolological Survey, 77/4, pp. 265–282.

McSween, M.Y., Jr. 1994: "What have we learned about Mars from SNC meteorites?". – Meteoritics, 29, pp. 757–779.
McSween M.Y., Jr., D. Stöffler 1980: Shock metamorphic features in ALHA 77005 meteorite. – Proceedings of 11th Lunar and Planetary Science Conference, pp. 717–719.
Melosh, H.J. 1984: Impact ejection, spallation, and the origin of meteorites. – Icarus, 59, pp. 234–260.
Mikouchi, T., M. Miyamoto 1998: Pyroxene and olivine microstructures in nakhlite Martian meteorites (abstract#1574). – 29th Lunar and Planetary Science Conference. CD-ROM.
Nyquist, L.E., D.D. Bogard, C.-Y. Shis, A. Greshake, D. Stöffler, O. Eugster 2001: Ages and geologic histories of Martian meteorites. – Chronological Evolution of Mars, 96, pp. 105–164.
Ostertag, R., G. Amthauer, H. Rager, H.Y. McSween Jr. 1984: Fe^{3+} in shocked olivine crystals of the ALHA77005 meteorite. – Earth and Planetary Science Letters, 67, pp. 162–166.
Puga, E., E. Jagoutz, J.M. Nieto, A. Diaz de Federico, M.D. Ruiz-Cruz 1998: On the origin of the brown color in ALHA 77005 olivine (abstract#1375). – 29th Lunar and Planetary Science Conference. CD-ROM.
Roberts, S., I. Beattie 1995: Micro-Raman spectroscopy in the Earth Sciences. – In: Potts, P.J., J.F.W. Bowles, S.J.B. Reed, M.R. Cave (Eds): Microprobe Techniques in the Earth Sciences, Chapman and Hall, London, pp. 387–408.
Stöffler, D. 1972: Deformation and transformation of rock-forming minerals by natural and experimental shock processes: I. Behaviour of minerals under shock compression. – Fortschritte der Mineralogie, 49, 50–113.
Stöffler, D. 1974: Deformation and transformation of rock-forming minerals by natural and experimental processes: II. Physical properties of shocked minerals. – Fortschritte der Mineralogie, 51, pp. 256–289.
Stöffler, D., A. Bischoff, U. Buchwald, A.E. Rubin 1988: Shock effects in meteorites. – In: Kerridge, J.F., M.S. Matthews (Eds): Meteorites and the Early Solar System, University of Arizona Press, Tucson, pp. 165–205.
Taylor, L.A., M.A. Nazarov, C.K. Shearer, H.Y. McSween, Jr., C.R. Neal, D.D. Badjukov, M.A. Ivanova, L.D. Barsukova, R.N. Clayton, T.K. Mayeda 2002: Martian meteorite Dhofar 019: A new Shergottite. – Meteoritics and Planetary Sciences, 37, pp. 1107–1128.
Treiman, A.H., M. McCanta, M.D. Dyar, C.M. Pieters, M.D. Hiroi Lane, J.L. Bishop 2006: Brown and clean olivine in chassignite from NWA 2737: Water and deformation (abstract#1314). – 37th Lunar and Planetary Science Conference. CD-ROM.
Yanai, K. 1979: Meteorite search in Victoria land, Antarctica in 1977–1978 Austral summer. – Mem. Natl. Inst. Polar Res., Spec. Issue, 12, pp. 1–8.
van de Moortéle, B., B. Reynard, P.F. McMillan, M. Wilson, P. Beck, P. Gillet, S. Jahn 2007: Shock-induced transformation of olivine to a new metastable $(Mg,Fe)_2SiO_4$ polymorph in Martian meteorites. – Earth and Planetary Science Letters, 261, pp. 469–475.
Walton, E.L., C.D.K. Herd 2007: Localized shock melting in lherzolitic Northwest Africa 1950: Comparison with Allan Hills 77005. – Meteoritics and Planetary Science, 42, pp. 63–80.